IOP PUBLISHING CLASSICAL AND QUANTUM GRAVITY

Class. Quantum Grav. **25** (2008) 184025 (10pp) doi:10.1088/0264-9381/25/18/184025

Visualizing gravitational-wave event candidates using the coherent event display

R A Mercer[1] **and S Klimenko**

University of Florida, PO Box 118440, Gainesville, FL 32611, USA

E-mail: ram@gravity.phys.uwm.edu

Received 21 April 2008, in final form 24 June 2008
Published 2 September 2008
Online at stacks.iop.org/CQG/25/184025

Abstract

As a worldwide network of gravitational-wave detectors is now operating with an unprecedented sensitivity it is becoming increasingly important to be able to easily visualize gravitational-wave event candidates from various search algorithms using these detector networks. The coherent event display (CED) has been developed with the goal of providing a simple and easy to use tool for performing follow up analyses of burst gravitational-wave event candidates. The CED produces a web page detailing reconstructed parameters, time–frequency maps, reconstructed detector responses, likelihood time–frequency maps and reconstructed parameter skymaps. The CED supports events from all 2, 3, 4 and 5 detector network combinations of the LIGO, GEO600 and Virgo detectors.

PACS numbers: 04.30.Db, 04.80.Nn, 07.05.Kf, 07.05.Rm, 95.30.Sf, 95.85.Sz

(Some figures in this article are in colour only in the electronic version)

1. Introduction

Over the past several years large scale laser interferometers have been used to search for gravitational waves (GW) at a sensitivity level where signals from distant astrophysical sources may be seen. There have been several joint data taking runs between the three detector, two site, LIGO [1] network, which has attained its design sensitivity, and the Virgo [2] and GEO600 [3] detectors, which are currently in the process of commissioning and are expected to achieve comparable sensitivities. It is therefore becoming increasingly important to be able to easily visualize, and study events from various search pipelines running on data from these detector networks.

One type of search that is being actively pursued is for unmodeled signals [4–7] that cannot be reliably searched for using matched filtering techniques. The coherent event display (CED)

[1] Present address: University of Wisconsin-Milwaukee, PO Box 413, Milwaukee, WI 53201, USA.

uses the search algorithms [8, 9] from the coherent wave burst (cWB) pipeline [10], which has been designed to search for these unmodeled, or 'burst', GW signals. The CED can therefore be used to investigate both burst GW event candidates, and accidental background events due to instrumental and environmental noise correlations by presenting reconstructed parameters, time–frequency maps, reconstructed detector responses and reconstructed parameter skymaps in a simple yet easy to use package.

Section 2 describes the different components that make up the CED, section 3 discusses the implementation and structure of the CED and finally in section 4 we summarize the main aspects of the CED.

2. Coherent event display output description

The coherent event display (CED) is split up into several sections detailing different aspects of the requested event. This section describes the contents of each of these sections. A complete description of all the parameters and plots contained within the CED can be found in the technical documentation [11].

2.1. Job and event parameters

The first two sections of the CED detail parameters specific to the analysis segment and the event in question. The GPS and UTC start times of the analysis segment used is reported along with parameters reconstructed using the cWB pipeline [8]. A description of some of these parameters can be found below.

- The CED reports the start, stop and central GPS times at which the requested event occurs, along with the central time relative to the start of the data segment used.
- As a measure of the strength of the event the CED reports the signal-to-noise ratio of reconstructed events and the strain amplitudes of the reconstructed detector responses.
- The main coherent statistic that the cWB algorithms, and hence the CED, uses to identify the events is the logarithm of the likelihood ratio (equation (16) in [8]). In the case of Gaussian quasi-stationary detector noise it can be written as

$$\mathcal{L} = \sum_{ij} \sum_{k=1}^{K} \frac{1}{\sigma_k^2[j]} [w_k^2[i, j] - (w_k[i, j] - \xi_k[\theta, \phi, i, j])^2], \tag{1}$$

  where the $\sigma_k^2[j]$ is the variance of the data from the kth detector at the frequency index j, the $w_k[i, j]$ are the wavelet amplitudes of the sampled detector data. The reconstructed detector responses $\xi_k[\theta, \phi, i, j]$ are the functions of the sky location and they are defined as

$$\xi_k = F_{k+} h_+ + F_{k\times} h_\times, \tag{2}$$

  where F_{k+} and $F_{k\times}$ are the antenna patterns of the kth detector for the plus (h_+) and cross ($h_\times$) GW polarizations respectively. The $\mathcal{L}$ is usually referred to as the likelihood functional. For burst sources the waveforms h_+ and $h_\times$ are not usually known but they can be estimated from the variation of the likelihood functional. The estimators of the h_+ and $h_\times$ are used for reconstruction of the detector responses, the likelihood matrix L_{nm} and the maximum likelihood ratio statistic

$$L = \sum_{m,n} L_{nm}, \tag{3}$$

  where n and m are the detector indices. More detailed description of the likelihood statistics and how they are calculated can be found elsewhere [8, 9].

- As a measure of the consistency of the event in different detectors the CED reports the network correlation coefficient. The likelihood, which has a meaning of the total normalized energy detected by the network, can be split up into two distinct types of energy

$$E_{\rm inc} = \sum_{n=m} L_{nm}, \qquad E_{\rm cor} = \sum_{n\neq m} L_{nm}, \tag{4}$$

  where the diagonal terms of the likelihood matrix ($m = n$) correspond to the incoherent energy, and the off-diagonal terms ($m \neq n$) correspond to the correlated energy. The network correlation coefficient is defined as

$$C_{\rm net} = \frac{E_{\rm cor}}{E_{\rm Null} + E_{\rm cor}}, \tag{5}$$

  where $E_{\rm Null}$ represents the total normalized energy of the reconstructed detector noise (see equation (12)). The network correlation, $C_{\rm net}$, is used to distinguish geniune GW signals from the environmental and instrumental artifacts. Usually, accidental coincidences are inconsistent between the detectors and they are reconstructed with the large value of the null energy resulting in the low value of the $C_{\rm net}$. Whereas for GW signals the $C_{\rm net}$ is close to unity.
- The reconstructed sky location for the event is recorded using ϕ and θ parameters. The coordinate frame used in the Earth fixed with $\phi = 0^\circ$ corresponding to the Greenwich Meridian, $\theta = 90^\circ$ corresponding to the equator and $\theta = 0^\circ$ corresponding to the North pole.

2.2. Time–frequency plots

The following section of the CED displays the time–frequency plots. They are shown for individual detectors and display the normalized wavelet amplitudes (see equation (13)) as a function of frequency and time. Also this section of the CED contains the likelihood time–frequency plot, where output of individual detectors are combined into the likelihood statistic calculated for each time–frequency location and maximized over the entire sky. Figure 1 shows an example likelihood time–frequency plot, created after running the CED on a 46–46 $M_\odot$ phenomenological [12, 13] binary black hole (BBH) injection.

The above likelihood time–frequency plot has been generated using the default 'pixel' plotting style. Two other plotting styles are available: 'shaded' which interpolates between adjacent data points to give a smoother appearance to the plot, and 'cluster' which reconstructs only the event cluster requested.

2.3. Reconstructed detector responses

The following section of the CED display plots shows the reconstructed detector responses. There are two types of plot, the first of which shows the reconstructed strain for the detected event, for each detector in the network in turn. These are calculated from the variation of the likelihood functional, equation (1), and an example, for the LIGO Livingston detector, can be seen in figure 2.

The other type of plot that the CED displays are reconstructed whitened waveforms superimposed with the detector output in units of the noise RMS.

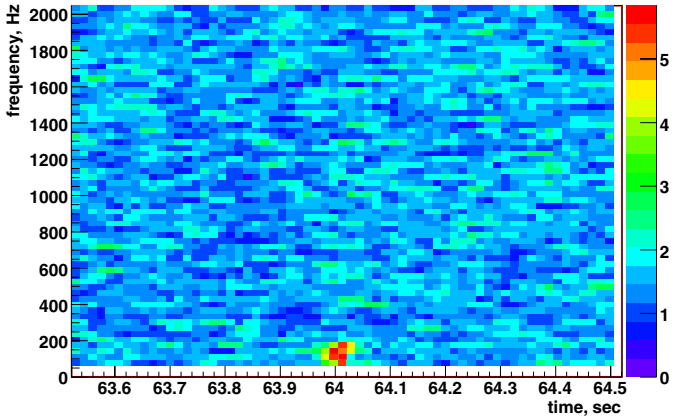

Figure 1. An example likelihood time–frequency plot from the coherent event display run on a 46–46 $M_{\odot}$ phenomenological BBH injection. High values of the likelihood correspond to the likely location of the event in the time–frequency domain. The injected event can be seen at a time of approximately 64 s and at a frequency of around 130 Hz.

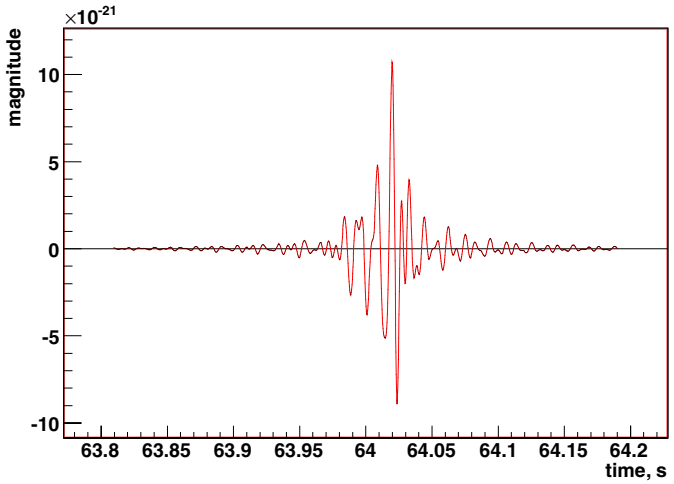

Figure 2. An example reconstructed strain signal plot showing the waveform reconstructed, for the LIGO Livingston detector, from running the coherent event display run on a 46–46 $M_{\odot}$ phenomenological BBH injection.

2.4. Skymaps

Several of the parameters reconstructed by the CED have a dependency on the sky location. These parameters are presented as a function of the sky location as a series of skymaps. The first two CED skymaps show the sensitivity of the detector network to the plus and cross polarizations. In order to understand what these skymaps represent, it is necessary to introduce the antenna pattern vectors, given in equation (6),

$$\mathbf{f}_{+(\times)}[i,j] = \left\{ \frac{F_{1+(\times)}[i,j]}{\sigma_1[j]}, \ldots, \frac{F_{K+(\times)}[i,j]}{\sigma_K[j]} \right\}. \tag{6}$$

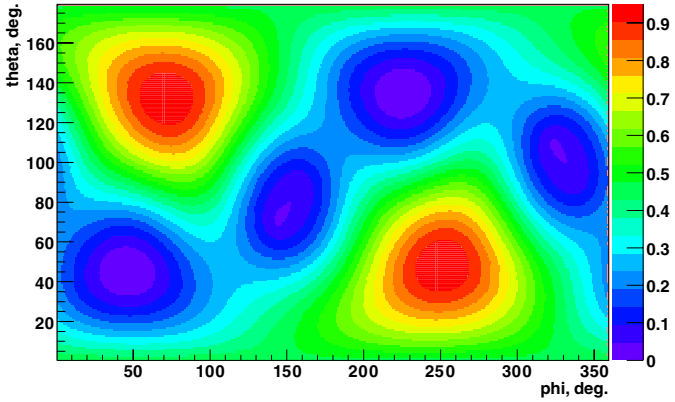

Figure 3. An example network sensitivity skymap showing the sensitivity of the detector network to the plus polarization for the LIGO detector network.

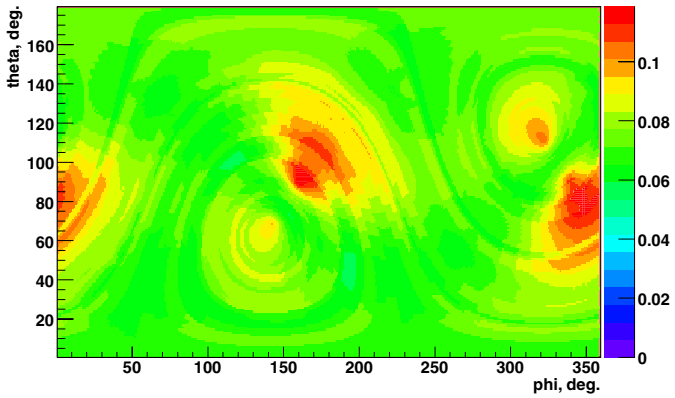

Figure 4. An example network sensitivity skymap showing the sensitivity of the detector network to the cross polarization for the LIGO detector network.

These antenna pattern vectors $\mathbf{f}_{+(\times)}[i, j]$ are defined in the dominant polarization frame [8] and the norms of these vectors $|\mathbf{f}_+|^2$ and $|\mathbf{f}_\times|^2$ represent the sensitivity of the detector network to the plus and cross polarizations respectively. An example plus polarization skymap, for the LIGO detector network, can be seen in figure 3. An example cross polarization skymap, also for the LIGO detector network, can be seen in figure 4.

As can be seen from figures 3 and 4 the two-site LIGO network is much less sensitive to the second polarization component $h_\times$, as is expected for the closely aligned detectors.

The next skymap shows the penalty factor which represents a constraint used in the coherent network analysis. The constraint requires the orthogonality of the reconstructed signal and noise and given in equation (7),

$$\Lambda_k = \sum_{ij} \left(w_k[i, j]\xi_k[i, j] - \xi_k^2[i, j] \right) = 0, \tag{7}$$

where $w_k[i, j]$ is the sampled detector data and $\xi_k[i, j]$ is the reconstructed detector response for the kth detector at time index i and frequency index j. The reason for this constraint is to

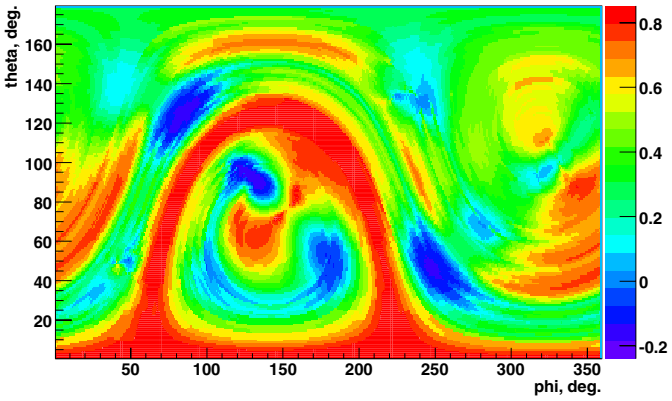

Figure 5. An example network correlation skymap that shows the value of network correlation coefficient, as a function of sky location, created after running the coherent event display on a 46–46 $M_{\odot}$ phenomenological BBH injection at a sky location of $\phi = 78^{\circ}$ and $\theta = 66^{\circ}$.

prevent the reconstruction of unphysical detector responses when the energy of the response S_k is greater than the total energy E_k in the detector data stream

$$E_k = \sum_{ij} w_k^2[i, j], \qquad S_k = \sum_{ij} \xi_k^2[i, j]. \tag{8}$$

This constraint (see equation (7)) is applied during the likelihood variation procedure of the cWB pipeline in the form of the penalty factor, by penalizing sky locations where this constraint is not satisfied, i.e.,

$$P_k = \begin{cases} \sqrt{E_k/S_k} & : \quad E_k < S_k \\ 1 & : \quad E_k > S_k, \end{cases} \tag{9}$$

where P_k is the penalty factor for the kth detector. The overall penalty factor P_f is given by the maximum value of P_k,

$$P_f = \max_k P_k. \tag{10}$$

It is this quantity P_f that is plotted as a function of sky location in order to generate the penalty factor skymap.

The next skymap shows the maximum value of the network correlation coefficient (see equation (5)) as a function of sky location. An example network correlation coefficient skymap can be seen in figure 5. One can see that the value of the C_{net} close to unity is achieved on the annulus in the sky reconstructed for the two-site LIGO network.

The likelihood approach [8] allows reconstruction of the source coordinates. However the maximum likelihood ratio statistic may not be the best statistic for this. As mentioned before (see the description of the penalty factor) it may achieve the maximum value at the sky location where unphysical estimators for h_+ and $h_\times$ are reconstructed. For more accurate estimation of the source coordinates we introduce the sky statistic

$$S_s = \mathcal{L} P_f C_{\text{net}}, \tag{11}$$

where $\mathcal{L}$ is the likelihood, P_f is the penalty factor (defined in equation (10)) and C_{net} is the network correlation coefficient (defined in equation (5)). An example sky statistic skymap for a simulated BBH signal injected at $\phi = 78^{\circ}$ and $\theta = 66^{\circ}$ can be seen in figure 6. High

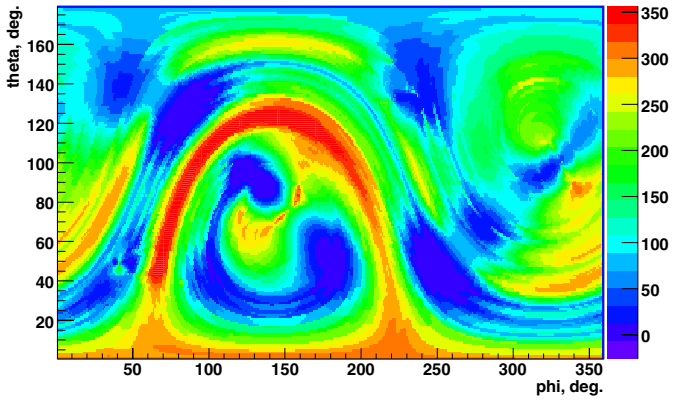

Figure 6. An example skymap showing the value of the sky statistic S_s, equation (11), as a function of sky location created after running the coherent event display on a 46–46 $M_\odot$ phenomenological BBH injection at a sky location of $\phi = 78^\circ$ and $\theta = 66^\circ$. High values of this parameter indicate the most likely sky location of a GW signal.

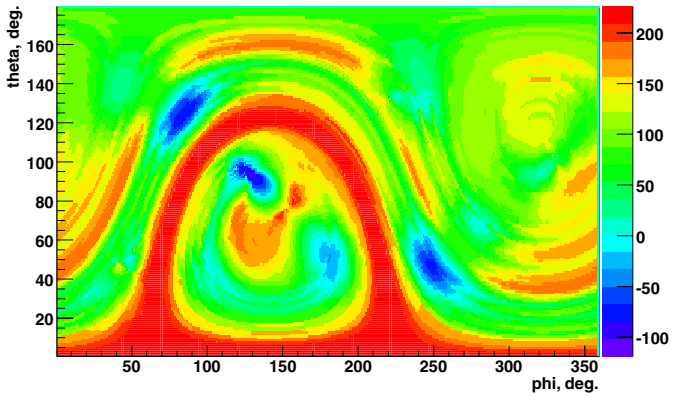

Figure 7. An example correlated energy skymap, showing the sum of the off-diagonal coefficients of equation (4), as a function of sky location, created after running the coherent event display on a 46–46 $M_\odot$ phenomenological BBH injection at a sky location of $\phi = 78^\circ$ and $\theta = 66^\circ$. The ring formed by high values of the correlated energy corresponds to an annulus in the sky with the same time delay between the two LIGO detector sites.

values of the sky statistic corresponds to the most likely sky location of a true GW signal and consistent with the injection coordinates.

As shown in equation (4) the total energy can be considered to be made of two components, $E_{\rm inc}$ the incoherent energy and $E_{\rm cor}$ the correlated energy. The next skymap shows the correlated energy $E_{\rm cor}$ as a function of sky location. An example correlated energy skymap can be seen in figure 7.

The maximum likelihood ratio statistic L has a meaning of the total reconstructed energy and can be written as $L = E - N$, where

$$E = \sum_{ij} |\mathbf{w}[i, j]|^2 , \qquad N = \sum_{ij} |\mathbf{w}[i, j] - \mathbf{s}[i, j]|^2 , \tag{12}$$

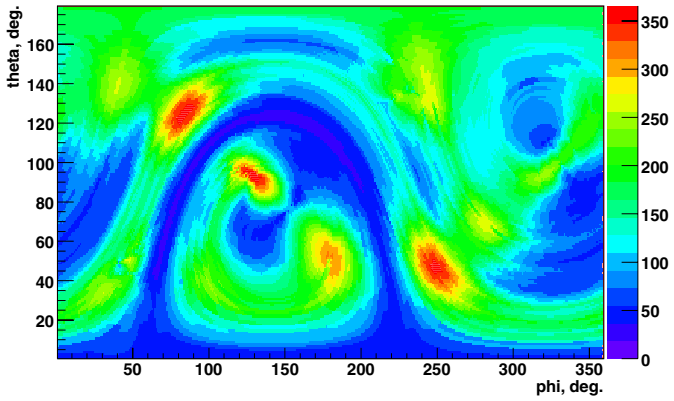

Figure 8. An example of the null energy skymap showing the value of the null stream, equation (12), as a function of sky location. The true sky location of the GW event is characterized by low values of the null energy. This example was created by running the coherent event display on a 46–46 $M_\odot$ phenomenological BBH injection at a sky location of $\phi = 78^\circ$ and $\theta = 66^\circ$.

where the vector $\mathbf{w}[i, j]$ is defined by

$$\mathbf{w}[i, j] = \left\{ \frac{w_1[i, j]}{\sigma_1[j]}, \ldots, \frac{w_K[i, j]}{\sigma_K[j]} \right\} \tag{13}$$

and the vector $\mathbf{s}[i, j]$ is defined by

$$\mathbf{s}[i, j] = \left\{ \frac{\xi_1[\theta, \phi, i, j]}{\sigma_1[j]}, \ldots, \frac{\xi_K[\theta, \phi, i, j]}{\sigma_K[j]} \right\}. \tag{14}$$

The quantity N is called the null stream and is plotted, as a function of sky location, on the null energy skymap. An example of such a skymap can be seen in figure 8. Low values of the null energy corresponds to the likely sky location of the GW signal in question.

As discussed earlier, one of the constraints that is applied during the analysis is the signal-to-noise orthogonality requirement given by equation (7). This constraint is applied to the likelihood by means of the penalty factor, equation (10). The energy disbalance skymap shows the sum, over detectors, of Λ_k as a function of sky location.

3. Implementation

The coherent event display (CED) is built on top of the coherent wave burst (cWB) algorithms and as such shares a lot of the properties of the main cWB search pipeline. This section briefly discusses how the CED is implemented using aspects of the cWB pipeline. Further discussion of the implementation can be found within the CED technical documentation [11].

3.1. Execution environment

The CED is controlled through a single driver script which ensures that the system environment is correctly setup so that the ROOT framework [14], the LIGO/Virgo frame library [15] and the wavelet analysis tool (WAT) [10] are available prior to starting the main analysis loop taken from the cWB pipeline.

Once it has been established that the execution environment is correctly setup the CED is started, details of the requested event are read in and an appropriate data stretch is determined and located.

3.2. Identifying the event

As the main analysis loop of the CED is the same as used in the cWB pipeline there may be multiple events detected in the chosen analysis segment. Only one of these events will be the requested event, it therefore needs to be determined which of these multiple events is the appropriate one.

This is done by stepping through the list of detected events and checking if the central time of the event, in each detector of the network, is contained within the range of times specified. If multiple events are found that match the supplied parameters then the CED chooses the event which has the highest likelihood, as it is more probably that this event will be of more interest.

3.3. Parameter, plot and website production

Once the requested event has been successfully identified all the appropriate parameters are recorded and the CED can now generate various plots illustrating the event, such as time–frequency maps, reconstructed detector responses and reconstructed parameter skymaps. Finally the end product of CED, a website, can be constructed.

4. Summary

In this paper, we have discussed the structure, layout and implementation of the CED and seen that it can be used for follow up analyses of both burst GW event candidates and accidental environmental or instrumental noise correlations. We have shown that the CED provides a simple, easy to use, tool that presents reconstructed parameters, time–frequency maps, reconstructed detector responses and reconstructed parameter skymaps in a single package.

Acknowledgments

The work was supported by the US National Science Foundation grant PHY-0555453 to the University of Florida, Gainesville, Florida.

References

[1] Sigg D (for the LSC) 2006 Status of the LIGO detectors *Class. Quantum Grav.* **23** S51
[2] Acernese F *et al* 2007 Status of Virgo detector *Class. Quantum Grav.* **24** S381
[3] Willke B (for the LSC) 2007 GEO600: status and plans *Class. Quantum Grav.* **24** S389
[4] Abbott B *et al* (LIGO Scientific Collaboration) 2004 First upper limits from LIGO on gravitational-wave bursts *Phys. Rev.* D **69** 102001
[5] Abbott B *et al* (LIGO Scientific Collaboration) 2005 Upper limits on gravitational-wave bursts in LIGO's second science run *Phys. Rev.* D **72** 062001 (*Preprint* gr-qc/0505029)
[6] Abbott B *et al* (LIGO Scientific Collaboration) 2006 Search for gravitational-wave bursts in LIGO's third science run *Class. Quantum Grav.* **23** S29 (*Preprint* gr-qc/0511146)
[7] Abbott B *et al* (LIGO Scientific Collaboration) 2007 Search for gravitational-wave bursts in LIGO data from the fourth LSC science run *Preprint* arXiv:0704.0943
[8] Klimenko S *et al* 2005 Constraint likelihood analysis for a network of gravitational wave detectors *Phys. Rev.* D **72** 122002
[9] Klimenko S *et al* 2008 A coherent method for detection of gravitational wave bursts *Class. Quantum Grav.* **25** 114029
[10] Klimenko S *et al* 2008 Coherent WaveBurst - WAT version 4.7.0, LIGO-T080011-00-Z

[11] Mercer R A and Klimenko S 2008 The coherent event display, LIGO-T080077-00-Z
[12] Ajith P *et al* 2008 A template bank for gravitational waveforms from coalescing binary black holes: I. Non-spinning binaries *Phys. Rev.* D **77** 104017 (*Preprint* arXiv:0710.2335)
[13] Brown D A *et al* 2007 Data formats for numerical relativity waves *Preprint* arXiv:0709.0093
[14] http://root.cern.ch
[15] http://lappweb.in2p3.fr/virgo/FrameL